Around and Around: An Investigation of Signals for Acoustic Position Estimation of Moving Objects

Florian Hammer, Markus Pichler, Harald Fenzl and Andreas Gebhard
Linz Center of Mechatronics, Linz, Austria
Email: florian.hammer@lcm.at

***Abstract*—Positioning methods have been investigated for decades now. Especially conditions like environmental noise and multipath propagation still drive the quest for robust methods that provide precise position estimates. Where radio frequency signals stumble, sound may succeed. Our approach to acoustic positioning is based on time-of-flight measurements utilizing the correlations of audible test signals and is based on a choice of system parameters that allow for robust positioning in harsh environments such as mines. Applying linear frequency chirp signals, we obtain a precision of position estimates in the millimeter range for stationary situations. However, as soon as the object under observation is in motion, its velocity causes the received test signals to be Doppler-shifted, and thus introduces a time-shift and a distortion in the respective correlation signals. In this contribution, we present a remedy to the Doppler shift problem by using pairs of hyperbolic chirp signals. We have investigated the performance of linear and hyperbolic chirp signals by employing them to estimate the position of a mobile tag which was moved on a circle at different levels of constant velocity. Our results illustrate that using single linear chirps, the position estimates describe a distorted circle due to the Doppler shift. Applying the hyperbolic chirp pair setup, we attain position estimates that are in alignment with the circular movement. In stationary scenarios, very high positioning precision in the range of 7 mm can be achieved down to a signal-to-noise ratio of -2.8 dB using the linear chirp signals. In situations of objects moving at a velocity of 1 m/s, the use of hyperbolic chirp signals leads to a precision of around 3 cm down to a signal-to-noise ratio of -3.2 dB.**

I. Introduction

The need for a method for the estimation of the position of an object under observation without contact gave rise to a variety of solutions so far. Wireless positioning systems range from optical over microwave-based to acoustic systems. The accuracy, as given by the mean position estimation error, and the precision, by means of the error's standard deviation, of a positioning system (cf. [1]) depend on the inherent system parameters, on the environment in which it is used and on the robustness of the system against potential disturbances such as noise, dust, and multipath propagation.

Throughout this paper, we present parts of the development of an indoor positioning system to be used in the harsh environment of mines. We were aiming at the system's capability of measuring the (2D) positions of miners within a radius of 10 m around a mining machine and their distances up to 50 m from the machine. We have decided to develop an acoustic positioning system based on time-of-flight (TOF) measurements applying correlation processing. Regarding the frequency range, the first choice would have been ultrasound due to its inaudibility. However, since the atmospheric sound attenuation in air increases with f^2, we decided to use measurement signals in the audible frequency range. A technical constraint was given by the limited power available at the miner's side which required the mobile tag to act as the receiver. The final system shall incorporate a total of six loudspeakers mounted around a machine and shall be robust against noise and multipath propagation.

This paper is structured as follows. Section II presents related work regarding indoor acoustic positioning. In sections III and IV, we describe our positioning method and the measurements we have carried out, respectively. The results of our measurements are presented in section V. Finally, we conclude our work in section VI.

II. Related Work

Wireless position estimation systems are mostly based on one of the following principles. In TOF/TOA (time-of-flight/time-of-arrival) systems, distances are determined by measuring the absolute time a signal takes from emission to reception, while TDOA (time-difference-of-arrival) systems measure the time differences of the signal arrival at three or more receivers. AOA (angle-of-arrival) systems measure the direction of propagation of a wave using an array of receiver sensors. Moreover, distances may be measured by calculating the received signal strength (RSS) at the receiver which allows for a distance estimation. From the distances, the position of the object is estimated. We refer to [1] for descriptions of wireless indoor positioning techniques and systems. As our system uses acoustic signals, we briefly review existing work in indoor acoustic positioning.

The *Cricket* system [2] determines the distances of a passive mobile tag, called listener, to reference points (beacons) by means of TOF measurements using ultrasonic signals. The Radio-Frequency (RF) signal pulses sent from the beacons contain beacon-specific information such as an ID and beacon coordinates, and trigger the acoustic measurements. From the distances of the tag to the Beacons, the tag may calculate its position considering the actual temperature as the speed of sound depends on the temperature (see below for details).

The position estimate is updated every second and reaches an estimation accuracy of about 10 cm.

The Active Bat system [3] is an ultrasound positioning system in which an ultrasound emitter is attached to an object, and receivers are mounted on the ceiling. TOF measurements to the nearest receivers are triggered via a wireless link. This system exhibits a 3D-accuracy of 3 cm for 95 % of the position readings.

In the next section, we present our method for acoustic position estimation.

III. Acoustic Positioning Method

A. Measurement Principle

Our method of position estimation is based on measurements of the times-of-flight $t_{\mathrm{TOF},1}$ and $t_{\mathrm{TOF},2}$ between two loudspeakers and a microphone that is mounted on the object to be located. From these TOF, the respective distances d_1 and d_2 are determined as

$$d = t_{\mathrm{TOF}} \cdot c_0, \tag{1}$$

where c_0 represents the speed of sound ($c_0 \approx 346$ m/s at a temperature of 24°C). Since the speed of sound depends on the actual temperature, as given in (2), we need to take the temperature into account when estimating distances and positions:

$$c_0 = 331.5 + 0.6 \cdot \vartheta \tag{2}$$

in m/s, where ϑ corresponds with the temperature in °C.

Given that the object remains on one side of the loudspeaker axis, the position can be estimated using bilateration. This principle is illustrated in Figure 1.

In the following, we present the measurement signals and describe the signal processing needed for the estimation of the object position from the recorded signal.

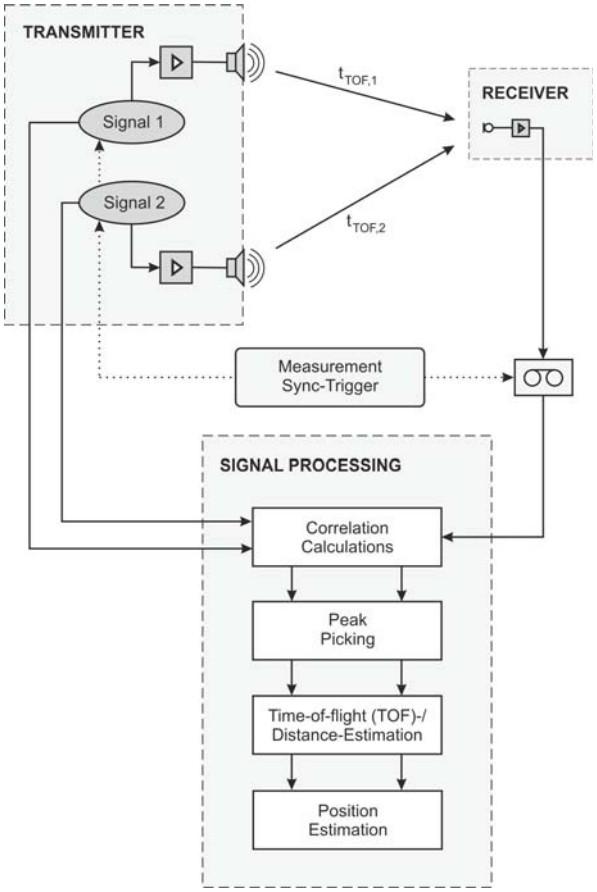

Fig. 1. Acoustic positioning principle. Two measurement signals are transmitted via loudspeakers, while, synchronously, the microphone signal at the receiver is recorded. From the correlation signals of the recorded signal with the original signals, the distances between the loudspeakers and the microphone can be calculated. Finally, the position of the microphone is estimated using bilateration.

B. Measurement Signals

Our first choice of a measurement signal was a linear frequency modulated (LFM) signal which provides high robustness against potential background noise. Equation 3 describes such a chirp signal $s_{\mathrm{LFM}}(t)$, where $W(t)$ represents a windowing function chosen to minimize spectral leakage outside the desired frequency band. Frequencies f_0 and f_1 denote the start and stop frequency, respectively, and T_s represents the duration of the signal.

$$s_{\mathrm{LFM}}(t) = W(t) \cdot \sin\left(2\pi\left(f_0 + \frac{f_1 - f_0}{2T_{\mathrm{s}}}t\right)t\right), \tag{3}$$

A frequency choice of $f_1 > f_0$ results in an up-chirp, and $f_1 < f_0$ results in a down-chirp signal. The LFM signals used in our system are applied in terms of one up-chip per loudspeaker channel operated at different start frequencies.

In situations of moving objects, we need to consider the frequency-shift that arises due to the Doppler-effect. Given that the sound source is stationary and the receiver is in motion at speed v, the Doppler-shifted received frequency f_{s} results from

$$f_{\mathrm{s}} = f_{\mathrm{b}} \cdot \left(1 + \frac{v}{c_0}\right), \tag{4}$$

where f_b denotes the original frequency of the transmitted signal.

As a consequence, if the object is moving, LFM signals are frequency-shifted which results in correlation signal distortions (cf. [4]), and thus in poor performance of the estimations of the distances, and the positions. Hence, we decided to test the employment of Doppler-tolerant measurement signals. Hyperbolic frequency modulated (HFM) signals exhibit optimum correlation performance at constant velocities [5]. In such situations (v = const.), the correlation peaks stemming from Doppler-shifted HFM signals are well-detectable compared to those of LFM signals (cf. [4]). Pairs of HFM chirps, i.e. an up-chirp and down-chirp signal emitted simultaneously, allow for the compensation of the Doppler-shift. A hyperbolic chirp

signal s_{HFM} is defined as follows ([5, 6]):

$$s_{\mathrm{HFM}}(t) = W(t) \cdot \sin\left(\frac{2\pi}{b}\ln\left(1 + bf_0 t\right)\right) \tag{5}$$

with

$$b = \frac{f_0 - f_1}{f_0 f_1 T_s}. \tag{6}$$

We have employed the HFM signals in pairs and different frequency sets per loudspeaker leading to a total of four correlation results.

We are aware of the fact that these configurations do not lead to a fair comparison of LFM (single chirp) and HFM (paired chirp) signals in the case of moving objects. However, our results are based on sequential development of our system, and they very well illustrate the effect of employing pairs of Doppler-invariant signals.

C. Signal Processing

This section describes the processing steps from correlation calculation to the computation of the object's position.

1) Correlation Processing: As soon as the microphone signal s_{r} of length T_{r} = 512 ms is recorded, its correlations $s_{\mathrm{c},p,q}$ with the zeropadded reference signals $s_{\mathrm{s},p,q}$ (two LFM and four HFM reference signals of length T_{s} = 360 ms) are derived employing Fast Fourier Transformations (FFTs) as given in (7).

$$s_{\mathrm{c},p,q} = \mathfrak{F}^{-1}\{\mathfrak{F}\{s_{\mathrm{r}}\}\mathfrak{F}\{s_{\mathrm{s},p,q}\}^*\}, \tag{7}$$

where $\mathfrak{F}\{s_{\mathrm{s},p,q}\}^*$ are conjugate complex Fourier transforms of the original chirp signals of channel p ($p \in \{1,2\}$), where q identifies the individual chirps per channel (LFM: $q = 1$, HFM: $q \in \{1,2\}$).

2) Peak-Picking and Distance Estimation: Each correlation signal $s_{\mathrm{c},p,q}$ is scanned for prominent peaks from which the TOF are estimated. Previous measurements have shown that a reflection may bring forth a higher correlation peak than the line-of-sight (LOS) signal. As to be able to deal with such situations, we determine the index of the maximum correlation value and pick a defined number of peaks between index zero and the maximum index applying peak-picking Algorithm 1.

The algorithm is given the maximum number of N_{pk} peaks to be picked and the threshold level s_{th} above which maxima are searched for. The input parameter $d_{\max}$ represents the maximum drop relative to the global maximum amplitude A_1 (e.g. $d_{\max}$ = 0.25), while parameter $d_{\min}$ defines the minimum amplitude level relative to peak amplitude A_k that is considered to belong to a single peak (e.g. $d_{\min}$ = 0.95), where index k denotes the actual peak number. The later feature helps dealing with double peaks. As a result of the peak-picking stage, we obtain the interpolated amplitudes $\hat{A}_{p,q}$ and interpolated correlation indizes $\hat{i}_{p,q}$ of the peaks found in the correlation signals.

Algorithm 1 Peak-picking algorithm

procedure PEAKFINDER($N_{\mathrm{pk}}, s_{\mathrm{th}}, d_{\min}, d_{\max}$)
  Define search interval as entire signal; k = 1
  while any value in $s_{\mathrm{c}} > s_{\mathrm{th}}$ and $k < N_{\mathrm{pk}}$ **do**
    Find maximum within search interval
    Discard peak if $A_k < d_{\max} \cdot A_1$ and exit
    Extend peak to the left and right until $A < d_{\min} \cdot A_k$
    Follow strictly monotonous slope to the left and right
    Estimate peak first (n_{c}) and second (n_{v}) moment about the mean
    Extend peak to a width of $3 \cdot n_{\mathrm{v}}$
    Follow strictly monotonous slope to the left and right
    Interpolate the peak maximum $\hat{A}_k$ and index $\hat{i}_k$ around the peak found
    Set peak area to zero
    Define search interval from 0 to i_k; k++
  end while
  return $\hat{A}$, $\hat{i}$
end procedure

From $\hat{i}_{p,q}$, we derive the TOF estimates

$$\hat{t}_{p,q} = \hat{i}_{p,q} \cdot \frac{1}{f_{\mathrm{s}}} \tag{8}$$

The TOF are derived from the peaks that are nearest to zero leading to $\hat{t}_{q,p}$. In the case of LFM chirps, the distances are simply estimated applying (1):

$$\hat{d}_{LFM,p} = \hat{t}_p \cdot c_0, \tag{9}$$

where p denotes the number of the channel.

In order to estimate the TOF and distances of the HFM chirp signals, we need to apply some more calculus to the TOF-pairs that resulted from the peak-picking:

$$\hat{\tau}_p = \frac{1}{2}\left(\hat{t}_{p,1} + \hat{t}_{p,2} - \hat{\phi}_p\left(\frac{1}{b_{p,2}f_{0,p,2}} + \frac{1}{b_{p,1}f_{0,p,1}}\right)\right) \tag{10}$$

with

$$\hat{\phi}_p = (\hat{t}_{p,2} - \hat{t}_{p,1})\left(\frac{1}{b_{p,2}f_{0,p,2}} - \frac{1}{b_{p,1}f_{0,p,1}}\right)^{-1}, \tag{11}$$

leading to an estimated distance of

$$\hat{d}_{\mathrm{HFM},p} = \hat{\tau}_p \cdot c_0. \tag{12}$$

3) Bilateration: Finally, the position of the object is estimated using bilateration, i.e. deriving the crossing position of the distance circles from each loudspeaker. First, the length of the base line l between the loudspeakers is calculated:

$$l = \sqrt{(y_{\mathrm{L2}} - y_{\mathrm{L1}})^2 + (x_{\mathrm{L2}} - x_{\mathrm{L1}})^2}, \tag{13}$$

where $(x_{\mathrm{L1}},y_{\mathrm{L1}})$ and $(x_{\mathrm{L2}},y_{\mathrm{L2}})$ represent the coordinates of loudspeakers 1 and 2, respectively. Applying the law of cosines, the estimated angle $\hat{\gamma}$ at the crossing of the distance circles towards the loudspeakers is derived as given in (14).

$$\hat{\gamma} = \arccos\left(\frac{l^2 + \hat{d_1}^2 + \hat{d_2}^2}{2 \cdot l \cdot \hat{d_1}}\right) \tag{14}$$

Finally, the estimated position coordinates $\hat{x}$ and $\hat{y}$ are calculated as

$$\hat{x} = x_{\mathrm{L1}} + \hat{d_1} \cdot \cos(\hat{\gamma}) \tag{15}$$

$$\hat{y} = y_{\mathrm{L1}} + \hat{d_1} \cdot \sin(\hat{\gamma}) \tag{16}$$

In the next section, we present the measurement setup and describe the scenarios we have tested.

IV. Measurements

A. Measurement Setup

As to be able to test the behavior of both the linear and the hyperbolic chirps, we have implemented them in our acoustic positioning system as illustrated in Figure 2.

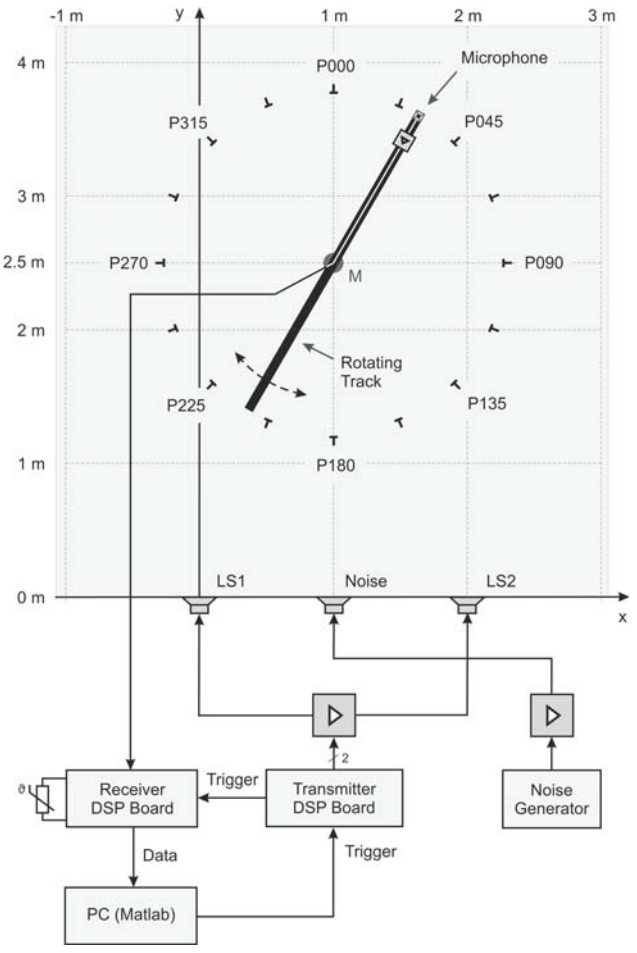

Fig. 2. Measurement setup applying a rotating beam. Upon a trigger from the measurement PC, the transmitter DSP board started to play out the measurement signals and simultaneously triggered the recording at the receiver DSP board. Moreover, the PC controlled the rotation speed of the beam.

As to keep the power consumption low, two low-power DSP boards[1] constituted the core of the transmitter and the receiver. Upon a trigger signal from a measurement PC the transmitter board synchronously started the playout of the measurement signals and triggered the recording of the microphone signal at the receiver.

The measurement signals were played out from the transmitter DSP board via an audio amplifier and two JBL 25AV loudspeakers. The signals emitted from LS1 and LS2 ranged from 6-11 kHz and 5-10 kHz, respectively, hence exhibiting a bandwidth of B = 5 kHz. The frequency ranges are overlapping as we aimed at the use of a total number of six different signals in the final system. The microphone signal was pre-amplified and captured at the receiver DSP board at a sampling frequency of f_{s} = 32 kHz as to keep the amount of data to be stored and processed as low as possible.

After the playout procedure, the DSP calculated the correlations between the recorded signal and the reference chirp signals and sent them to the PC. In each measurement, the temperature value was measured for the calculation of the actual speed of sound. In the post-processing stage, we applied the peak-picking algorithm to the correlation results. The algorithm was set as to pick a maximum of six peaks given a threshold value of ten times the median of the correlation signal.

In order to be able to carry out measurements of circular microphone movement at defined velocities, we mounted a wooden beam on a turn table which was electronically driven and controlled via the PC. The microphone consisted of three electret microphones that were tightly fixed together in angles of 120° as to obtain a high microphone signal level and an omnidirectional pattern. This microphone construction was attached to the outer end of the beam (cf. Figure 2). We have chosen to use a beam radius of r = 1.27 m as for the microphone to move along a circumference of 8 m. This setup alleviated the adjustment of the microphone's velocity. Both the loudspeakers and microphone operated at a height of 1.79 m. Marks on the floor (cf. Figure 2) were used for the microphone adjustment in the stationary measurement scenarios.

The test signals' duration was T_{s} = 360 ms, while the signal recorded via the microphone was T_{r} = 512 ms long ($T \approx T_{\mathrm{s}} + \frac{50\ \mathrm{m}}{340\ \mathrm{m/s}} = 147$ ms, rounded up as to correspond to an FFT-frame size of 16,384). All chirp signals were linearly faded in and out by 10 ms, constituting a trapezoidal windowing function $W(t)$. A summary of the measurement parameters is given in Table I.

In our PeakFinder algorithm, we have set the following parameters: $N_{\mathrm{pk}} = 6$, threshold $s_{\mathrm{th}} = 10 \cdot \tilde{s}_{\mathrm{c}}$, minimum drop $d_{\mathrm{min}} = 0.95$, and maximum drop $d_{\mathrm{max}} = 0.25$.

As we aimed at testing the positioning system at different levels of signal-to-noise-ratio (SNR), white noise was played

[1] TI TMS320C5515 eZdsp USB, including stereo audio codecs.

TABLE I
SYSTEM SETUP PARAMETERS.

Chirp parameters Signal 1	f_0 = 6 kHz f_1 = 11 kHz
Chirp parameters Signal 2	f_0 = 5 kHz f_1 = 10 kHz
Signal length: transmitted recorded	T_s = 360 ms T_r = 512 ms

via an amplifier and another loudspeaker that was arranged between the main loudspeakers. The maximum sound pressure level (SPL) of the noise signal was 98 dB at position P180 (as depicted in Figure 2). Based on recordings of the chirp signals at position P180, the SNR levels of the LFM and HFM signals were derived and are given in Table II. Note that the SNR values of the HFM conditions are higher because the HFM signals were sent in pairs.

TABLE II
SIGNAL-TO-NOISE-RATIO (SNR) AT DIFFERENT LEVELS OF WHITE NOISE.

Level	SNR_{LFM} (dB)	SNR_{HFM} (dB)
1	-22.3	-13.6
2	-12.0	-3.2
3	-2.8	5.9
4	7.2	16.0
5	22.7	31.4

Both kinds of chirp signals were tested under stationary conditions and in scenarios in which the tag was moved in a circle at a constant velocity. The following two sections describe these measurement scenarios.

B. Stationary Tag Scenarios

In the first part of our measurements, we set the tag microphone to stationary positions (P000, P090, P180, P270, cf. Figure 2) and carried out ten measurements per signal per position. The microphone position was adjusted perpendicular to reference marks on the floor.

C. Moving Tag Scenarios

The second part of our measurements comprised the study of the LFM and HFM signals in cases of object movement. After starting the rotating beam and accelerating it to the defined tag velocity, 31 measurements have been carried out per scenario. The LFM and HFM signals were tested at velocities of 0.5 m/s and 1.0 m/s in clockwise and counter-clockwise direction.

We measured the ground truth of the position of the microphone by attaching a plate below the turn table on which we drew a clock-like 16-unit scale and by placing a mark at the bottom side of the beam at the microphone's side. During each measurement, the rotation of the beam around the scale was filmed (bottom-up) using a digital camera. The videos were later analyzed. From the beam angles transcribed at the instants of measurement, i.e. in the middle of the chirps, we have derived the positions of the microphone.

V. RESULTS

A. Stationary Measurements

Figure 3 presents the results of the stationary measurements using both LFM (+) and HFM (*) chirp signals.

These results are apparently biased due to the inaccuracies that arose from the determination of the microphone's real position by using a perpendicular. Irrespective of the bias, we observed the following:

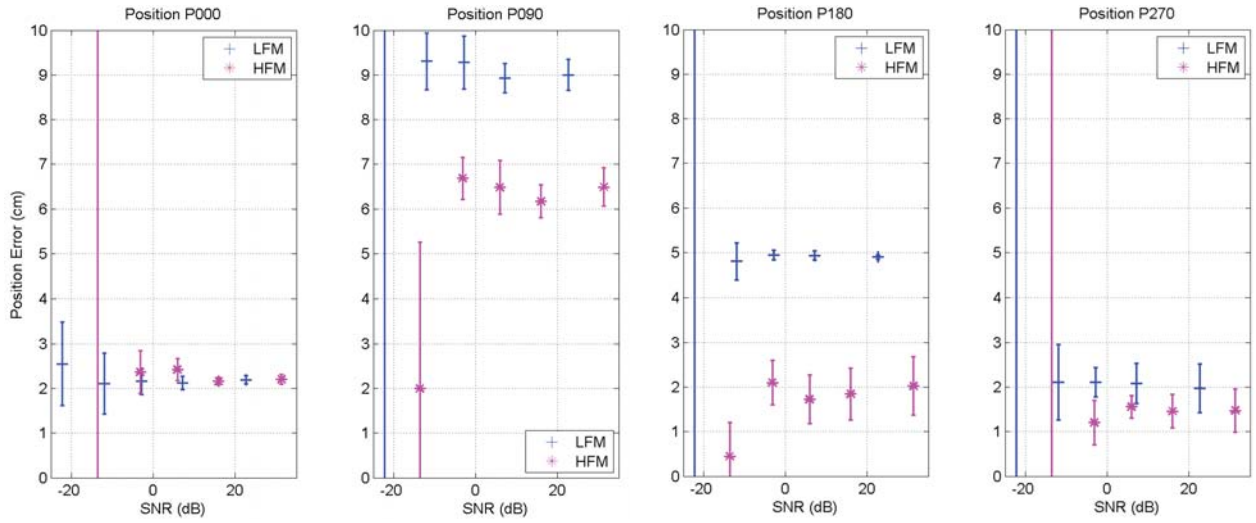

Fig. 3. Position errors vs. SNR of LFM (+) and HFM (*) signals at positions P000 to P270. The results are apparently biased due to inaccuracies in the ground truth data. However, the precision lies below 7 mm down to an SNR of -3.2 dB.

- Starting from high SNR values the deviations of the (biased) accuracy lie below 1 cm down to an SNR of around -3.0 dB.
- The precision of the LFM signals is especially exceptionally low at positions P000 and P180 ($\sigma < 2$ mm), while at the positions that do not lie on the symmetric axis between the loudspeakers, i.e. P090 and P270, LFM and HFM signals result in about the same precision of below 7 mm.
- In the stationary scenarios, the LFM signals seem to be more robust against noise. This may be due to the fact that only one distance estimation is needed per channel. The necessity of deriving two correlations and combining them in order to obtain the TOF seems to make HFM position estimates more sensitive to noise.

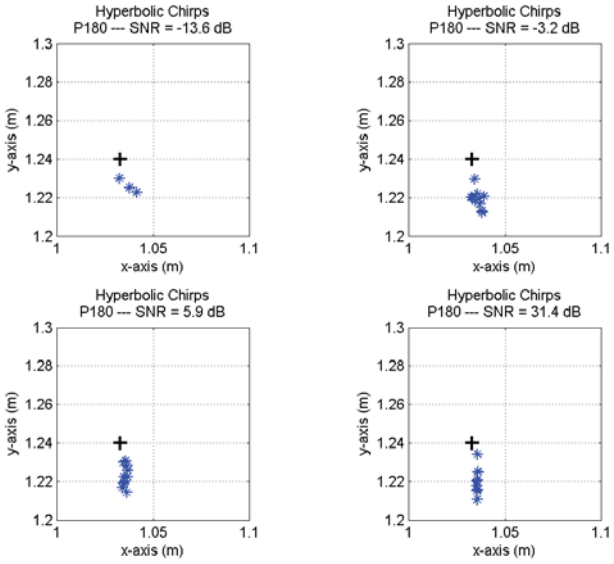

Fig. 4. Position estimates at position P180 at four SNR levels resulting from stationary measurements using HFM chirps. The results are biased but exhibit high precision. Similar results were obtained using the LFM signals.

Figure 4 illustrates the measurement results obtained around position P180 using HFM signals. The use of LFM signals led to very similar results. The deviations of the position estimates result from the fact that the position marks were made on the floor while the microphone was attached to the rotating beam at a height of 1.79 m. Hence, it is difficult to set the microphone to exactly the same position in a reproducible way. This being said, the results of both the LFM signals and the HFM signals, suggest a high level of precision. At a high SNR, the precision is in the range of 0.2 mm horizontally for both LFM and HFM signals, and about $\sigma_{\mathrm{v,LFM}} = 4$ mm and $\sigma_{\mathrm{v,HFM}} = 6.7$ mm vertically. An increasing noise level (decreasing SNR) leads to a steady increase of the horizontal deviation, however remaining as low as $\sigma_{\mathrm{h,LFM}} = 1.1$ mm at an SNR of -2.8 dB and $\sigma_{\mathrm{h,HFM}} = 2.2$ mm at an SNR of -3.2 dB.

In both cases, the sets of position estimates lie along a vertical line in the scenarios of high SNR, and they hardly exhibit any deviation in the horizontal direction. As the position estimates are aligned in a straight vertical line, the TOF/distance variation was equal for each channel (LS1/LS2). This variation may have arisen from the fact that the receiver DSP board is triggered by the transmitter DSP board via a general-purpose-input-output pin, and that the timing between the measurement trigger and the instant of recording the microphone signal is not deterministic but exhibits a certain delay jitter. The delay jitter may result from the fact that the audio signal is sampled at a frequency of f_{s}=32 kHz, i.e. every 31.25 µs. At position P180 and at a speed of sound of about 345 m/s, this results in a distance deviation of

$$\Delta d_{1,2} \approx \frac{345 \text{ m/s}}{32 \text{ kHz}} \approx 11 \text{ mm} \tag{17}$$

for both distances (symmetric position between the loudspeakers). Projected to the vertical axis, the deviation makes 13.6 mm which is about twice the measured vertical standard deviation of 6.7 mm.

B. Moving Receiver Measurements

1) Linear Chirps: Figure 5 presents the position estimates of the LFM system at a tag velocity of v = 0.5 and 1.0 m/s and an SNR of -2.8 dB. This Figure clearly illustrates the impact of the Doppler-shift on the position estimates. The Doppler-shift causes a time-shift, and thus prolongs or shortens the measured distance. The direction of the shift depends on the direction of the tag and on the slope of the chirp (up or down). The amount of the distance shift depends on the velocity of the tag. Hence, the pattern of the estimates as shown in Figure 5 varies with velocity and direction.

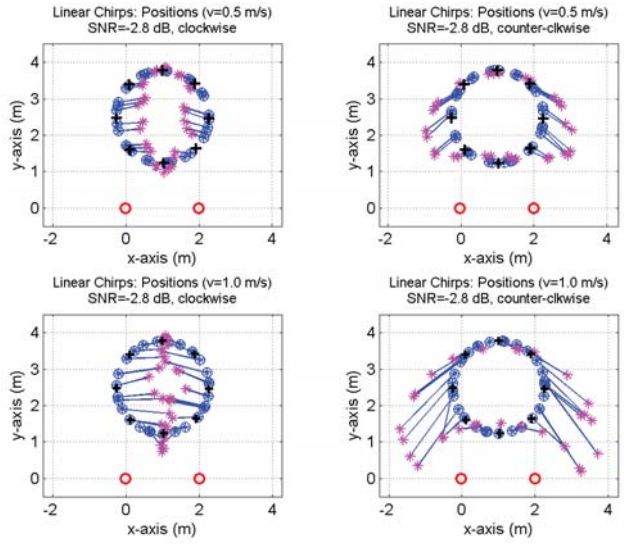

Fig. 5. Position estimates using one LFM up-chirp signal per loudspeaker at an SNR of -2.8 dB. The top plots give the results for a velocity of 0.5 m/s in clockwise and counter-clockwise direction, while the bottom plots show the estimates for a velocity of 1.0 m/s. These figures very well illustrate the impact of the Doppler-shift on the position estimates. The red circles denote the loudspeakers.

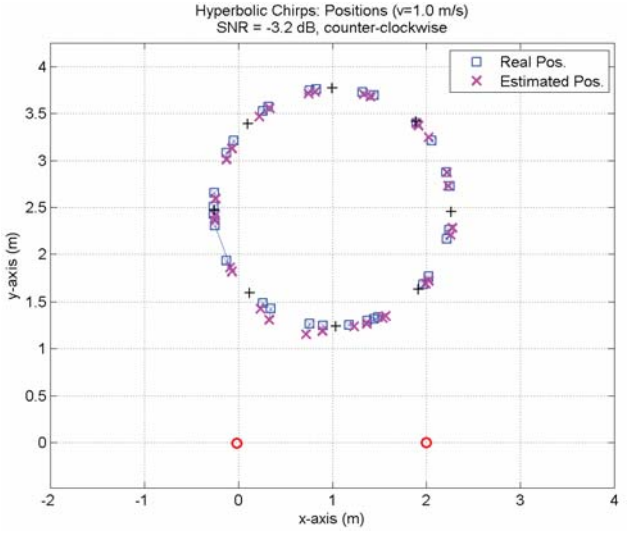

Fig. 6. Position estimates of the system based on hyperbolic (HFM) chirps at the tag moving counter-clockwise at a speed of 1.0 m/s and an SNR of -3.2 dB. The red circles denote the loudspeakers.

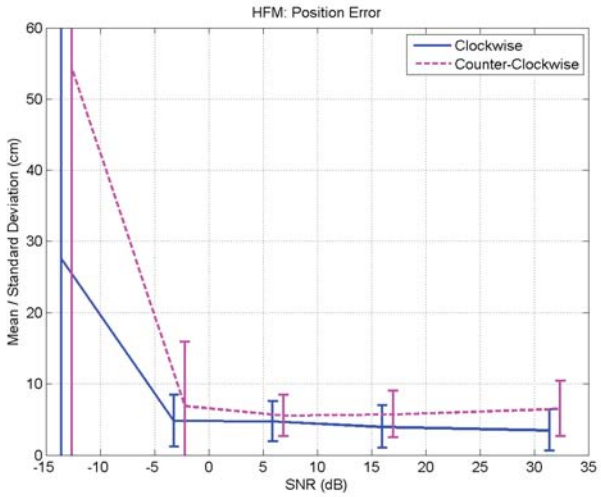

Fig. 7. Position estimation errors vs. SNR using HFM signals at a velocity of 1 m/s for clockwise direction (solid) and counter-clockwise direction (dashed).

The variation of the pattern results from the fact that the individual distances from the object to the loudspeakers are shortened or extended depending on the Doppler-shift. A higher velocity leads to larger distance variations, and thus to a stronger distortion of the pattern. An inversion of the direction leads to an inversion of the effect of the Doppler-shift on the distance variation. Hence, the patterns for clockwise and counter-clockwise movement differ.

2) Hyperbolic Chirps: Figure 6 presents the position estimates of the HFM system at a tag velocity of v = 1.0 m/s, counter-clockwise, and an SNR of -3.2 dB. The plot illustrates the advantage of using pairs of HFM signals. While HFM signals themselves result in accurate estimates of the distances of moved tags due to their Doppler-invariance regarding the correlation signals, the pairing of the chirp signals compensates for the shifts of the estimated distances (cf. Equations 10 and 12).

The means and standard deviations of the position estimation errors of the latter scenario are given in Figure 7. The solid line (blue) illustrates the results for the clockwise direction while the dashed line depicts the results for the counter-clockwise direction. In this configuration, the positioning accuracy remains below 7 cm down to an SNR of -3.2 dB, while the precision of the position estimates lies between 3 and 4 cm. At the lowest SNR-level of -13.6 dB, 70 % of the position estimates remain below a position error of 12 cm.

VI. Conclusions

We have presented an acoustic positioning system based on time-of-flight measurements which operates in the audible domain. Our system was designed to allow for robust position estimation in mines by using frequency-modulated signals, and by estimating distances based on correlation processing including a peak-picking algorithm.

In laboratory measurements, we have tested the use of single linear frequency-modulated (LFM) and paired hyperbolic frequency-modulated (HFM) signals for determining the position of stationary and mobile tags. In the stationary scenarios, our system provides an precision in the range of 7 mm down to an SNR level of -2.8 dB using LFM signals. In the scenario of a tag moving at a velocity of 1 m/s, the application of HFM chirp pairs leads to a precision of around 3.5 cm at an SNR of -3.2 dB.

Compensating the position deviations due to the low sampling rate by measuring the time lag between the trigger slope and the actual sampling of the acoustic signal may improve the precision of the position estimates.

The pros and cons of our audible acoustic positioning system may be summarized as follows.

+ Higher accuracy and precision compared to RF positioning resulting from a high ratio of bandwidth to propagation speed.
+ Simple system concept.
+ Low-power receiver electronics.
+ Direct sampling of the measurement signals allows for robust correlation processing.
+ Application of a peak-picking algorithm is possible. Enables effective multipath mitigation.
+ RF noise and propagation conditions do not disturb the acoustic measurement procedure.
+ Audible frequency waves are less attenuated than ultrasound waves, and thus allow for long range measurements.
o Speed of sound is a function of the temperature and needs compensation.

– Acoustic noise and room-acoustics need to be considered.
– Low measurement rate of about 1 Hz, resulting from signal length (time-bandwidth product, maximum distance), low propagation speed, and limited processing power.

Future work includes the implementation of several mobile tags that return the correlation peak results for position estimation via a wireless link instead of a cable.

ACKNOWLEDGEMENTS

The work presented in this paper has been carried out as a part of the project FEATureFACE funded by the European Research Fund for Coal and Steel (RFCR-CT-2012-00001). It has partially been supported by the Austrian COMET-K2 programme of the Linz Center of Mechatronics (LCM), and was funded by the Austrian federal government and the federal state of Upper Austria. The authors would like to thank Clemens Hesch and Veronika Putz for their support.

REFERENCES

[1] Hui Liu, Houshang Darabi, Pat Banerjee, and Jing Liu. Survey of wireless indoor positioning techniques and systems. *IEEE Transactions on Systems, Man, and Cybernetics-Part C: Applications and Reviews*, 37(6):1067–1080, November 2007.

[2] Nissanka Bodhi Priyantha. *The Cricket Indoor Location System*. PhD thesis, Department of Electrical Engineering and Computer Science, Massachusetts Institute of Technology, June 2005.

[3] Mike Addlesee, Rupert Curwen, Steve Hodges, Joe Newman, Pete Steggles, Andy Ward, and Andy Hopper. Implementing a sentient computing system. *IEEE Computer*, 34(8):50–56, August 2001.

[4] J. Yang and T. K. Sarkar. Doppler-invariant property of hyperbolic frequency modulated waveforms. *Microwave and Optical Technology Letters*, 48(6):1174–1179, June 2006.

[5] Jan J. Kroszczynski. Pulse compression by means of linear-period modulation. *Proceedings of the IEEE*, 57(7):1260–1266, July 1969.

[6] Xiufeng Song, Peter Willett, and Shengli Zhou. Range bias modeling for hyperbolic-frequency-modulated waveforms in target tracking. *IEEE Journal of Oceanic Engineering*, 37(4):670–679, October 2012.